Geotechnical Aspects of Underground Construction in Soft Ground – Zhou, Guan & Li (eds)

Effect of infill nonlinearity on frame response to tunnelling

Y. Yu
College of Civil Engineering, Qilu Institute of Technology, Jinan, China

A. Franza
Department of Civil and Architectural Engineering, Aarhus University, Aarhus, Denmark

L. Neves & A.M. Marshall
Department of Civil Engineering, University of Nottingham, Nottingham, UK

ABSTRACT: Tunnel construction is needed for infrastructure development in urban areas. However, underground excavation can detrimentally influence adjacent buildings; in particular, for framed structures with shallow foundations, damage would localise in the infill walls. This paper uses a two-stage analysis method (TSAM) to evaluate the effect of infill nonlinearity on the frame response to tunnelling. First, TSAM results are validated using centrifuge experimental and advanced numerical results. Then, the influence of the infill nonlinearity on the foundation displacements and building deformation parameters are analysed, considering both long and short structures. During this stage, the reinforced concrete (RC) frame and the endwall are modelled as elastic, while both elastic and advanced constitutive models are adopted for the masonry infills. Finally, the role of infill nonlinearity in frame shear and bending behaviours is investigated.

Keywords: Finite element modelling, infilled frame, tunnelling, soil-structure interaction, two-stage analysis method

1 INSTRUCTION

Rapid urbanisation has resulted in the increased demand for constructing underground transport systems. An increasing number of tunnels are excavated around or beneath existing surface structures and buried foundations. The excavation of the soil will cause ground movements as well as stress relief, which may adversely affect the surrounding structures. Inevitably, the tunnel, soil and the existing structure will interact with each other, which is known as tunnel-soil-structure interaction (TSSI).

Reinforced concrete (RC) frame structures are recognised as one of the most common structural forms of buildings worldwide. In practice, frame response to tunnelling is generally analysed by simplifying it as an equivalent elastic beam or plate (Franzius et al. 2006; Pickhaver et al. 2010; Farrell et al. 2014), although the structural characteristics have been shown to significantly affect the frame response to tunnelling (Boldini et al., 2018; Elkayam and Klar, 2019; Franza and DeJong, 2019). The response of bare frames to tunnelling while considering structural details has been investigated through numerical modelling (Boldini et al., 2018; Boldini et al., 2021; Goh and Mair, 2014) and experimental methods (Xu et al., 2020). In addition, Son (2015) adopted elastic bricks and inelastic brick-mortar joints in the 2-D Universal Distinct Element Code. Franza et al. (2022) investigated the response of frame structures with elastic infills to tunnelling. However, the nonlinear behaviour of infills has received limited attention in previous studies (Fu et al., 2018).

DOI: 10.1201/9781003413790-26

Various researchers have employed a two-stage analysis method (TSAM) to investigate the TSSI problem (Deck and Singh, 2012; Franza et al., 2022; Selby, 1999; Elkayam and Klar, 2019; Haji et al., 2018; Franza and DeJong, 2019). In the first stage, greenfield displacements, acquired either empirically or through analytical means, are applied to an elastic soil model in the absence of the structure to calculate the reaction forces of the soil caused by tunnelling; in the second stage, the computed reaction forces are applied to the soil with the structure in place. This method allows for the efficient and acceptably accurate simulation of tunnelling-induced building response without considering the complex soil nonlinear behaviour and advanced constitutive models.

The aim of this paper is to investigate the effect of the nonlinearity of infills on the global behaviour of infilled frame structures subjected to tunnelling, adopting the TSAM analysis method within the Finite Element Method (FEM) software Abaqus (Simulia, 2010). First, the tunnelling-induced bare frame response obtained using the TSAM are validated by comparison against published experimental (Xu. et al., 2020) and numerical results (Boldini et al., 2021). The TSAM approach is then used to investigate the effect of infill nonlinearity on the soil-structure interactions, for both short and long frames. Results indicate the significant underestimation in terms of building shear response and vertical displacements of the foundation when adopting an elastic model for the frame infills compared to a more realistic nonlinear model.

2 BUILDING DEFORMATION PARAMETERS

Building deformation parameters were reported by Son and Cording (2005), Ritter et al. (2020) and Xu et al. (2020) to evaluate the building distortions under the shear, bending and axial modes caused by tunnelling. Figure 1 shows the parameter definitions using four corner points of a single unit of the frame building.

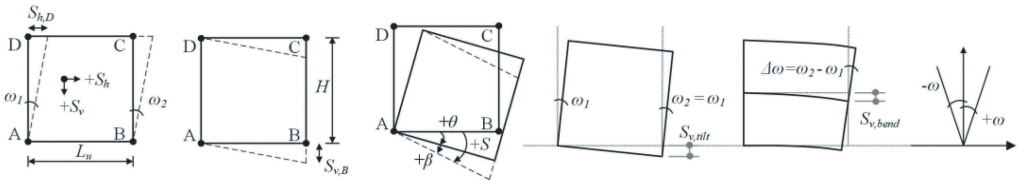

Figure 1. Building deformation parameters in bays and sign convention (after Ritter et al., 2020).

The building response to tunnelling was quantified based on the horizontal S_h and vertical S_v displacements of the corner points, the building unit height H, and the building unit length L_u.

Base horizontal strain:

$$\varepsilon_{h,base} = \frac{S_{h,B} - S_{h,A}}{L_u} \tag{1}$$

Top horizontal strain:

$$\varepsilon_{h,top} = \frac{S_{h,C} - S_{h,D}}{L_u} \tag{2}$$

The angular distortion β was expressed by the subtraction of tilt θ from slope S:

$$\beta = S - \theta = S - \frac{\omega_1 + \omega_2}{2} = \frac{S_{v,B} - S_{v,A}}{L_u} - \frac{(S_{h,C} - S_{h,B}) + (S_{h,D} - S_{h,A})}{2H} \tag{3}$$

where ω_1 and ω_2 are in radians. The angular distortion β, which is equal to shear strain when using the method of Son and Cording (2005); Ritter et al. (2020); Xu et al. (2020), relates to the level of building shear distortion and its shear response, whereas the curvature relates to the bending contribution of the building response (Ritter et al., 2020).

In addition, as done by Ritter et al. (2020), it can be informative to decompose the total vertical displacements of each building bay as:

$$S_{v,total} = S_{v,B} - S_{v,A} \tag{4}$$

where A and B are the nodes at the bottom corners of a given bay, into those caused by tilt $S_{v,tilt}$, shear $S_{v,shear}$, and bending $S_{v,bend}$, so as to distinguish the role of each mechanism. The value of $S_{v,tilt}$ is defined as:

$$S_{v,tilt} = \omega_1 L_u \tag{5}$$

The value of $S_{v,bend}$ is defined as:

$$S_{v,bend} = \chi \frac{L_u^2}{2} = \Delta\omega \frac{L_u}{2} \tag{6}$$

where χ is the average curvature and $\Delta\omega = \omega_2 - \omega_1$. Positive values imply a hogging mode. The sum of $S_{v,tilt}$, $S_{v,shear}$ and $S_{v,bend}$ gives total vertical displacement:

$$S_{v,total} = S_{v,tilt} + S_{v,shear} + S_{v,bend} \tag{7}$$

It should be noted that the parameters β and $S_{v,shear}$ represent the building shear response while χ and $S_{v,bend}$ mainly indicate the building bending behaviour.

3 TSAM VALIDATION - BARE FRAME SCENARIO

The TSAM results in modelling the bare frame response to tunnelling are validated using the centrifuge tests conducted by Xu et al. (2020), as well as numerical modelling results by Boldini et al. (2021) and Franza et al. (2022) for the same scenario; the advanced SANISAND model was used to replicate soil behaviour and implemented within Abaqus and Plaxis 3D, respectively. The experiments were performed using Leighton Buzzard Fraction *E* silica sand with a soil relative density of I_d = 90%. A plane strain setup was used, incorporating a flexible cylindrical membrane tunnel filled with water. The centrifuge test labelled as F2t3b6L is considered as the validation case. The layout of the bare frame building is plotted in Figure 2. In the prototype scale of the centrifuge tests, the tunnel has a diameter of D_t = 6.1m, and a cover depth of C = 8m (C/D_t = 1.3). The entire frame structure has a transverse width of B = 31.3m, with each bay having a width of b_{bay} = 5.2m. The height of each storey is h_{storey} = 2.7m, and the thickness of each floor and foundation is equivalent to t = 0.22m. All the TSAM simulations consider the structure standard weight case.

According to the numerical model parameters from Boldini et al. (2021) and Franza et al. (2022), the TSAM model adopted an elastic frame with Young's modulus of E = 53.8GPa, a Poisson's ratio of ν = 0.334, and a unit weight of γ = 27 kN/m^3. Franza et al. (2022) also adopted an analytical two-stage method (results omitted), assuming for the elastic continuum a Young's modulus of E_s = 45MPa and a Poisson's ratio of ν = 0.3. To simulate the soil-frame interaction, a friction coefficient of μ_{soil} = 0.625, corresponding to the critical state friction of the soil, was used. The soil was assumed to have zero tensile strength. The greenfield vertical and horizontal displacements provided by Boldini et al. (2021) at the soil surface were fitted as input data in the TSAM model. These displacements were obtained at tunnel volume losses of $V_{l,t}$ = 1% and 2%.

Figures 3a to d show the vertical and horizontal displacements at the foundation base and the underlying soil from the centrifuge tests, advanced numerical results, and the TSAM results, all with tunnel volume loss of $V_{l,t}$ = 1% and 2%. The TSAM model demonstrates a satisfactory replication of the foundation and underlying soil displacements observed in the centrifuge tests and advanced numerical simulations, both in the vertical and horizontal

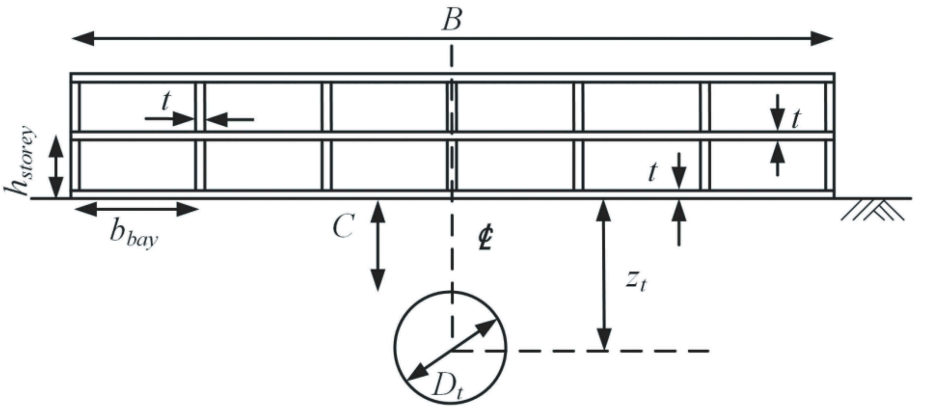

Figure 2. Layout of bare frame building in validation case.

directions. However, the numerical data, including both results from Boldini et al. (2021), Franza et al. (2022) and the TSAM analysis, slightly underestimate the vertical deformations of the foundation observed in the centrifuge tests at $V_{l,t}$ = 1% and overestimate the vertical displacements of the frame at $V_{l,t}$ = 2%. In the meantime, the horizontal displacements predicted at the foundation base are negligible in both centrifuge and numerical results; the level of slippage between the foundation and the soil is well captured in the TSAM. The comparison of the maximum angular distortion β_{max} (sign was not considered) is shown in Figure 3e. The numerical results, including both the advanced numerical model and the TSAM model, show a tendency to underestimate β_{max} at $V_{l,t}$ = 1%. The TSAM results exhibit good agreement with experimental results at $V_{l,t}$ = 2%, when the formation of a gap influences the induced distortions. Overall, the TSAM modelling satisfactorily replicates the frame response to tunnelling. Interestingly, there is a difference in predicted settlements of the building (as well as greenfield conditions) by Boldini et al. (2021) and Franza et al. (2022), despite the fact that they used a identical advanced soil constitutive model. This indicates that a simple

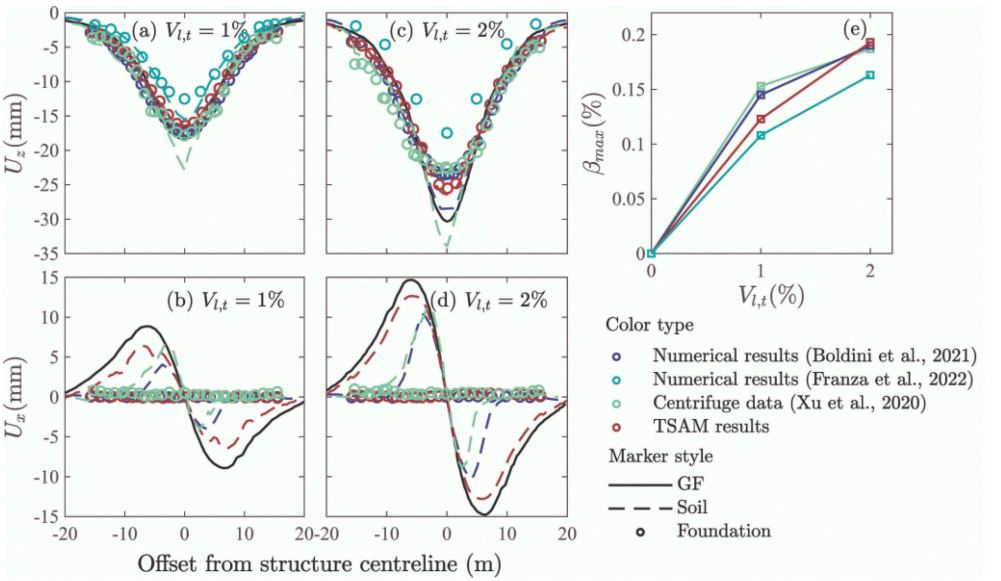

Figure 3. Validation of TSAM results on (a)-(d): vertical U_z and horizontal U_x displacements, and (e): maximum frame distortion.

TSAM may, in certain cases, benefit the analysis of tunnelling-induced soil-structure interaction since it provides a unique input (greenfield displacements), ensuring the focus is on the effect of structural features.

4 RESPONSE OF INFILLED FRAMES TO TUNNELLING

4.1 *Model details*

The frame structure in this study is based on the prototype-scale model of in-plane centrifuge tests conducted by Xu et al. (2020) and includes the masonry infills, focusing on assessing the impact of infill nonlinearity on the frame response to tunnelling. The short building consists of three bays with a transverse length (B) of 15.64 m, while the long building has six bays with B = 31.06 m. Both buildings have a height above ground level (H) of 5.46 m, a raft foundation, a slab, and column thickness of 0.22 m, and a building width (L) of 8.66 m. Each bay is divided by a column and has a length (b) of 5.19 m. All the scenarios considered in this study have the same dimension for the openings with a width of 1 m and height of 1.4 m. For the case where the tunnel is constructed directly beneath the structure with e = 0, the entire short frame scenario is located in the sagging zone; the sagging length (B_{sag}) equals the building transverse length of 15.64 m. In contrast, the long frame building has a sagging length (B_{sag}) of 25.1 m and a hogging length (B_{hog}) of 5.96 m. To reduce computational cost and focus on the in-plane strain behaviour, only half of the structure is modelled along the longitudinal direction of the tunnel.

The greenfield with a tunnel volume loss of $V_{l,t}$ = 3%, represented by a Gaussian curve, is obtained by doubling greenfield profiles corresponding to $V_{l,t}$ = 1.5% from Yiu et al. (2017) (Figure 4). The whole soil-structure system (soil, frame, lintel and endwalls) is assumed elastic except for the masonry infill walls. The elastic properties of different components in the soil-frame system are presented in Table 1. The masonry infills are simulated as isotropic linear elastic within the yield surface, with a perfectly plastic post-yield response. A modified Concrete Damaged Plasticity (CDP) model (CDP model with infinite compressive strength) is adopted for the infill simulation (Yiu et al., 2017). This CDP * model is defined by σ_c = infinite, σ_t = 0.5 MPa, ψ= 36.9°, the flow potential eccentricity ε (Abaqus default value of 0.1 adopted here), ratio of initial equi-biaxial compressive yield stress to initial uniaxial compressive yield stress σ_{b0}/σ_{c0} (Abaqus default value of 1.16 adopted here), and dimensionless parameter K that controls the shape of the yield surface (Abaqus default value of 0.67 adopted here) (Kupfer and Gerstle, 1973; Richart et al., 1928).

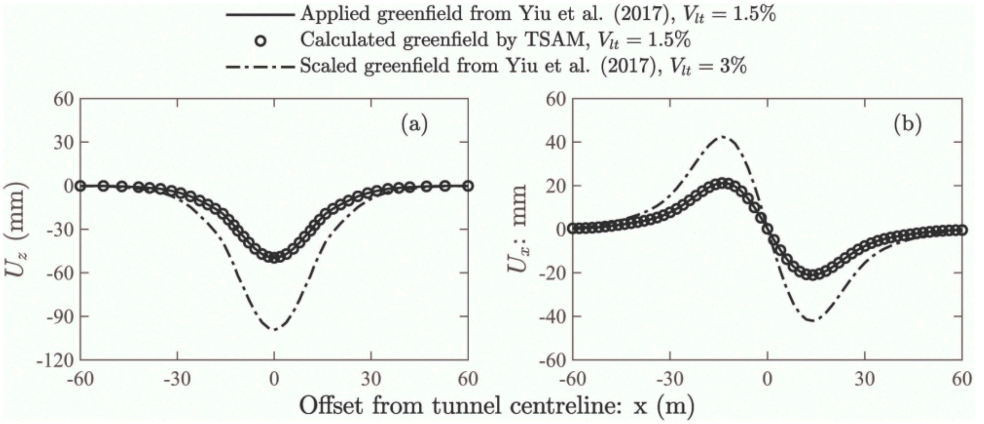

Figure 4. Validation of TSAM results on maximum frame distortion.

Table 1. Elastic properties of soil-frame structure system.

Elements	γ (kN/m^3)	E (GPa)	v (-)
Soil	19.5	0.02	0.35
Frame	27	53.8	0.33
Lintel	13	9	0.2
Endwall	13	4	0.2
Infill wall	13	4	0.2

Notes: γ = density; E = Young's modulus; μ = Poisson's ratio.

A three-dimensional ten-node quadratic tetrahedron continuum element (C3D10) is employed to model the entire soil-frame system. The displacements of the soil bottom boundary are fixed in all directions, while displacements are restrained perpendicular to the vertical planes at the sides of the model. Additionally, this study utilises a frictional interface implemented as a surface-to-surface contact with finite sliding formulation in ABAQUS. The shear behaviour at these interfaces follows the basic isotropic Coulomb friction model, with the soil-frame interface adopting a frictional coefficient μ_{soil} = 0.3 (Fu et al., 2018) and the frame-infill contact using μ_{infill} = 0.7 (Wu et al., 2022). The structure is positioned at the tunnel centreline with zero eccentricity.

4.2 *Effect of infill nonlinearity*

Figure 5 compares vertical (U_z) and horizontal (U_x) displacements of the frame foundations and the soil for short and long frames. In both CDP * and elastic models: (i) notable changes in soil deformation slopes occur at foundation edges for both U_z and U_x in both frame scenarios due to the higher stiffness of the structure compared to the soil; (ii) long structures exhibit considerably smaller vertical displacements (Figure 5a) compared to short structures, indicating that increased transverse width reduces maximum settlements for structures with zero eccentricity; (iii) the gap between the foundation and underlying soil is more pronounced in long frames; (iv) sliding occurs in both short and long buildings, but horizontal displacements at the foundation base are negligible, demonstrating the raft foundation's effectiveness in resisting horizontal ground movements due to high axial stiffness. These findings align with prior studies by Xu et al. (2020), Boldini et al. (2021), and Goh and Mair (2011). Additionally, the elastic model yields smaller vertical displacements and larger soil-foundation gaps compared to the CDP * model, particularly in long frames (Figure 5a). The difference in horizontal displacements between the elastic and CDP * models is negligible (Figure 5b). These

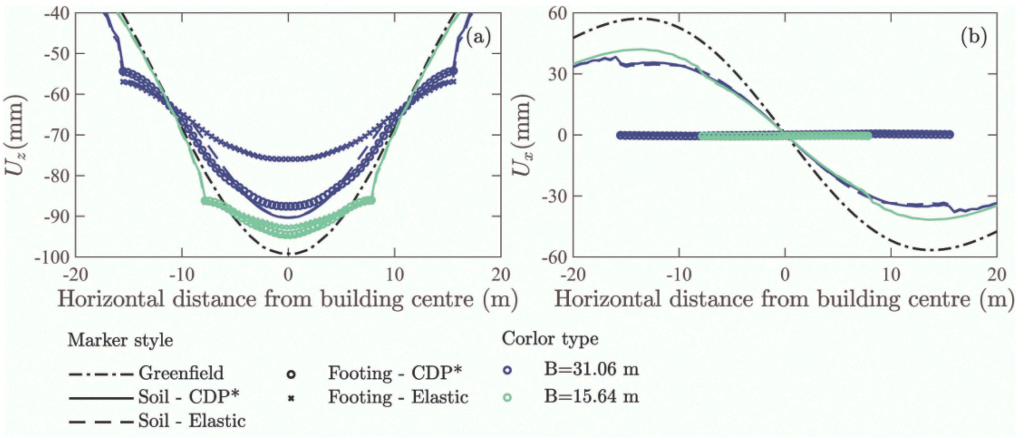

Figure 5. Comparison of footing base and underlying soil displacements with different building transverse widths, (a) vertical displacements and (b) horizontal displacements (upward in vertical and right in horizontal means positive).

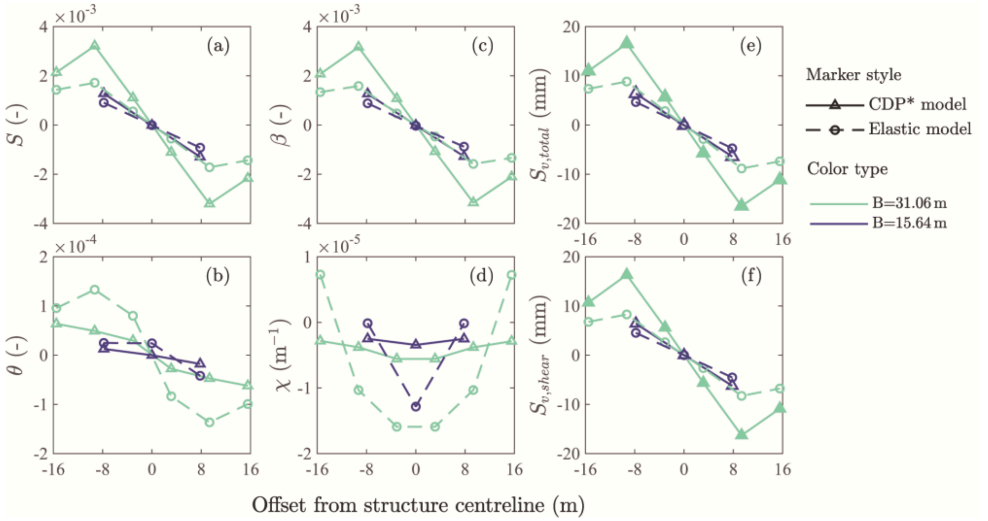

Figure 6. Building deformation parameters along building bays with different building transverse widths when $e = 0$: (a) slope, (b) tilt, (c) angular distortion, (d) curvature, (e) total vertical deflection and (f) vertical deflection caused by shear.

observations highlight the importance of accounting for infill nonlinearity when assessing building responses to tunnelling (when tunnelling induces relatively large settlements).

The comparison of building deformation parameters between short and long frames is illustrated in Figure 6. When the building eccentricity is zero, tilt ($S_{v,tilt}$) is minimal and the bending response for a frame structure is negligible, the vertical deflections primarily result from shear ($S_{v,total} \approx S_{v,shear}$). (i) The slope ($S$) and angular distortion (β) trends caused by the CDP * model are similar in both buildings, with the long building showing higher magnitudes, especially near inflection points. (ii) The largest tilt (θ) occurs at frame edges for both models in both scenarios, with the long frame showing higher values near inflection points. (iii) The long frame exhibits greater building curvature (χ) when using the elastic model, with the highest values near the building centre. (iv) The elastic model results in larger building tilt and curvature but underestimates building slope and angular distortion compared to the CDP *model. (v) Figure 6e and f reveal that vertical settlements in the infilled frame building are primarily due to shear deformation, with bending contributing negligibly. (vi) For the long building in sagging and hogging areas, the largest $S_{v,total}$ and $S_{v,shear}$ magnitudes occur near inflection points. Figure 6 shows that wider building transverse width leads to the increased shear response whereas the elastic model significantly underestimates the overall deflection (mainly caused by shear) caused by tunnelling. These results highlight the importance of considering infill nonlinearity for accurately assess the building behaviour during tunnelling.

5 CONCLUSIONS

This study numerically investigated the effect of infill nonlinearity on the frame response to tunnelling, taking into account the structure's transverse length. A two-stage analysis method (TSAM) was implemented in ABAQUS, adopting the elastic model for soil and the reinforced concrete frame, and both elastic and CDP* models for the infills. Tunnelling-induced foundation displacements and building deformation parameters along frame bays were analysed. It was demonstrated that the elastic model underestimates the shear and total vertical displacements of the building. Results highlight the significant influence of infill nonlinearity on the behaviour of the frame structure, particularly for relatively long frames spanning across both sagging and hogging regions.

REFERENCES

Boldini, D., Losacco, N., Bertolin, S., & Amorosi, A. 2018. *Finite Element modelling of tunnelling-induced displacements on framed structures*. Tunnelling and Underground Space Technology, 80 (April):222–231.3

Boldini, D., Losacco, N., Franza, A., DeJong, M., Xu, J., & Marshall, A. 2021. *Tunneling-induced deformation of bare frame structures on sand: Numerical study of building deformations*. Journal of Geotechnical and Geoenvironmental Engineering, 147(11).

Boscardin, M. D. & Cording, E. J. 1989. *Building response to excavation-induced settlement*. Journal of Geotechnical Engineering, 115(1):1–21.

Deck, O. Singh, A. 2012. A*nalytical model for the prediction of building deflections induced by ground movements*. International Journal for Numerical and Analytical Methods in Geomechanics, 36(1):62–84.

Elkayam, I. & Klar, A. 2019. *Nonlinear elastoplastic formulation for tunneling effects on superstructures*. Canadian Geotechnical Journal, 56(7):956–969.

Farrell, R., Mair, R., Sciotti, A., & Pigorini, A. 2014. *Building response to tunnelling*. Soils and Foundations, 54(3):269–279.

Franza, A. DeJong, M. J. 2019. *Elastoplastic solutions to predict tunneling-induced load redistribution and deformation of surface structures*. Journal of Geotechnical and Geoenvironmental Engineering, 145(4):04019007.

Franza, A., Miraei, S., Boldini, D., Losacco, N. 2022. *An equivalent beam approach for assessing tunnelling-induced distortions of frames with infills*. Tunnelling and Underground Space Technology, 129:104686.

Franzius, J. N., Potts, D. M., & Burland, J. B. 2006. *The response of surface structures to tunnel construction*. Proceedings of the Institution of Civil Engineers-Geotechnical Engineering, 159(1):3–17.

Goh, K. H. & Mair, R. J. 2014. *Response of framed buildings to excavation-induced movements*. Soils and Foundations, 54(3):250–268.

Goh, K. & Mair, R. J. 2011. *Building damage assessment for deep excavations in Singapore and the influence of building stiffness*. Geotechnical Engineering, 42:1–12.

Haji, T. K. et al. 2018. *Mixed empirical-numerical method for investigating tunnelling effects on structures*. Tunnelling and Underground Space Technology, 73:92–104.

Kupfer, H. B. & Gerstle, K. H. 1973. *Behavior of concrete under biaxial stresses*. Journal of the engineering mechanics division, 99(4):853–866.

Pickhaver, J. & Pickhaver, J. 2006. *Numerical modelling of building response to tunnelling*. PhD thesis, Oxford University, UK.

Richart, F. E., Brandtzæg, A., & Brown, R. L. 1928. *A study of the failure of concrete under combined compressive stresses*. Technical report, University of Illinois. Engineering Experiment Station. Bulletin; no. 185.

Ritter, S. et al. 2020. *Building deformation caused by tunneling: Centrifuge modeling*. Journal of Geotechnical and Geoenvironmental Engineering, 146(5):04020017.

Selby, A. 1999. *Tunnelling in soils–ground movements, and damage to buildings in Workington, Uk*. Geotechnical & Geological Engineering, 17(3-4):351–371.

Simulia, D. S. 2010. *Abaqus analysis user's manual*. Dassault Systemes, Pawtucket, USA.

Son, M. (2015). *Response analysis of nearby structures to tunneling-induced ground movements in sandy soils*. Tunnelling and Underground Space Technology, 48:156–169.

Son, M. Cording, E. J. (2005). Estimation of building damage due to excavation-induced ground movements. Journal of geotechnical and geoenvironmental engineering, 131(2):162–177.

Wu, J.-R., Di Sarno, L., Freddi, F., & D'Aniello, M. 2022. *Modelling of masonry infills in existing steel moment-resisting frames: Nonlinear force displacement relationship*. Engineering Structures, 267:114699.

Xu, J., Franza, A., & Marshall, A. M. 2020. *The response of framed buildings on raft foundations to tunneling*. Journal of Geotechnical and Geoenvironmental Engineering.

Yiu, W. N., Burd, H. J., Martin, C. M. 2017. *Finite-element modelling for the assessment of tunnel-induced damage to a masonry building*. Geotechnique, 67(9):780–794.